

---

## Supporting Information

# High Safety and Long-Life Silicon-based Lithium-ion Batteries via a Multifunctional Binder

Hua Liu,<sup>†, §</sup> Tongqing Chen,<sup>†, §</sup> Zhixin Xu,<sup>‡</sup> Zuozhen Liu,<sup>†, #</sup> Jun Yang,<sup>‡, \*</sup> Jianding Chen<sup>†, \*</sup>

<sup>†</sup>School of Materials Science and Engineering, East China University of Science and Technology, Shanghai 200237, China.

<sup>‡</sup>Shanghai Electrochemical Energy Devices Research Center, School of Chemistry and Chemical Engineering, Shanghai Jiao Tong University, Shanghai 200240, China.

<sup>#</sup>Sino Polymer Co., Ltd., Shanghai 200237, China.

Corresponding Authors

\*E-mail: yangj723@sjtu.edu.cn

\*E-mail: jiandingchen@ecust.edu.cn

<sup>§</sup>H. Liu and T. Chen contributed equally to this work.

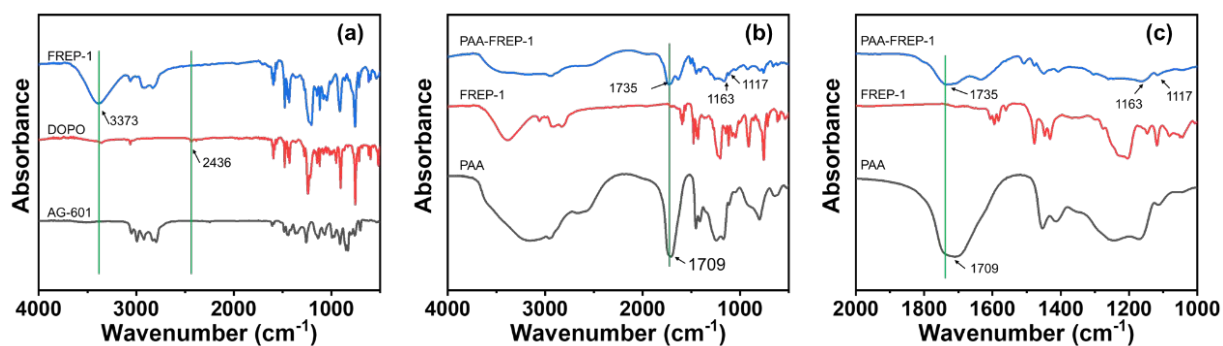


**Figure S1.** (a) FTIR spectra of AG-601, DOPO and FREP. (b) FTIR spectra of PAA, FREP and PAA-FREP. (c) Enlarged detail in the range of 1000-2000  $\text{cm}^{-1}$  of (b).

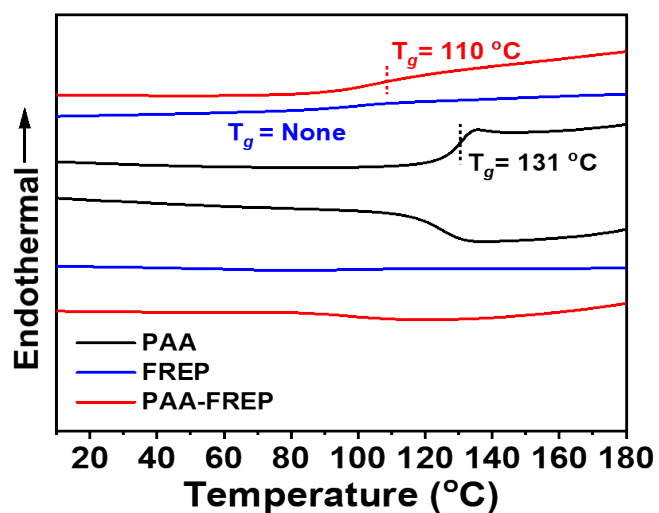


**Figure S2.** Differential scanning calorimetry (DSC) of PAA, FREP and PAA-FREP ( $10^{\circ}\text{C min}^{-1}$ ).

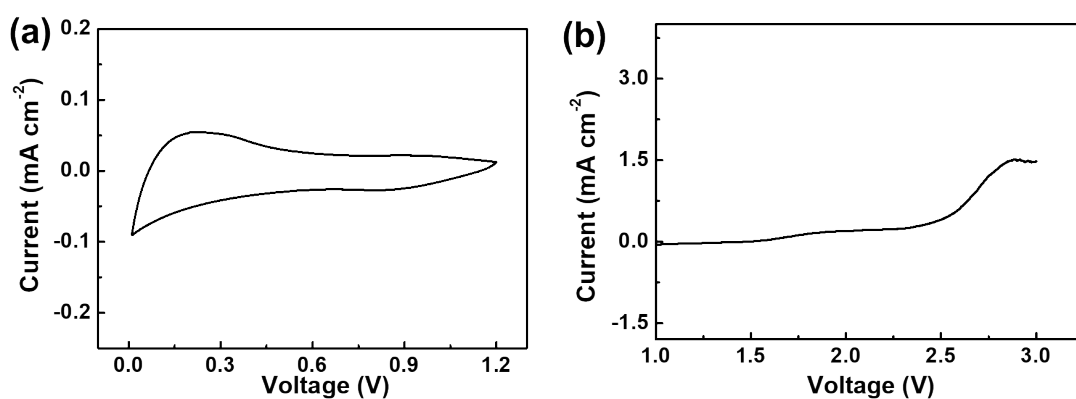


**Figure S3.** (a) Cyclic voltammetry of PAA-FREP from 0.01 V to 1.2 V. (b) Linear sweep voltammetry of PAA-FREP from 1.0 V to 3.0 V. The electrodes were composed by PAA-FREP, and Super P conductive carbon with a mass ratio 1:1.

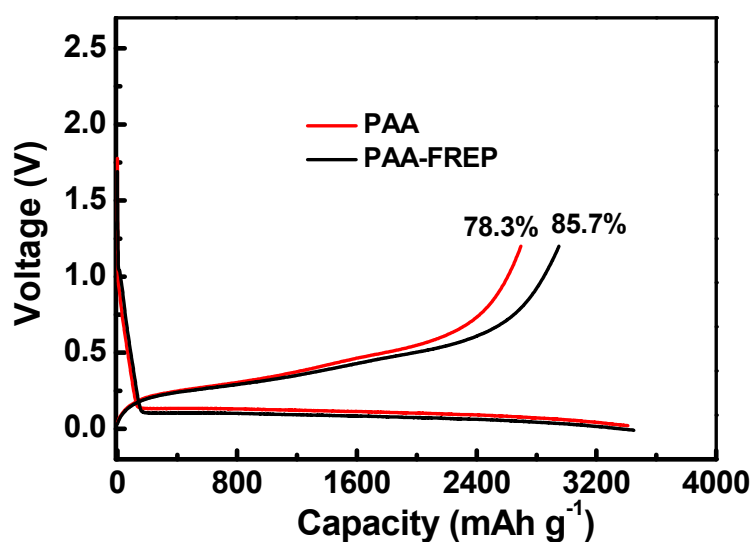


**Figure S4.** Voltage profiles and the initial Coulombic efficiencies of SiNPs electrodes with PAA-FREP and PAA binders cycled at 0.1 A g<sup>-1</sup>.

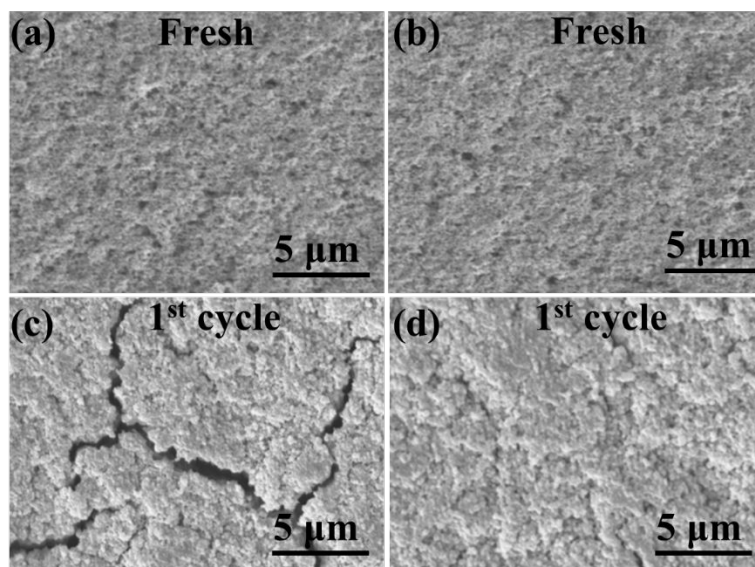


**Figure S5.** SEM images of SiNPs electrodes with different binders. (a) PAA and (b) PAA-FREP binders before cycling, (c) PAA and (d) PAA-FREP binders after the first cycle.

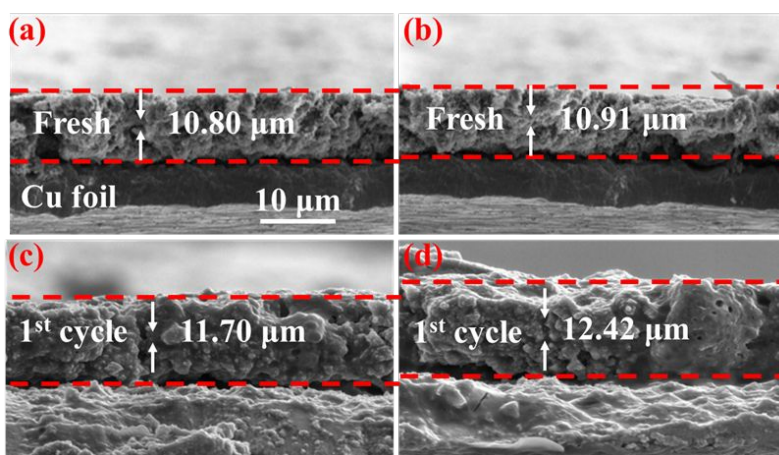


**Figure S6.** Cross-sectional SEM images of SiNPs electrodes before (upper) and after (lower) first cycle. Using PAA-FREP (left) and PAA (right) binders.

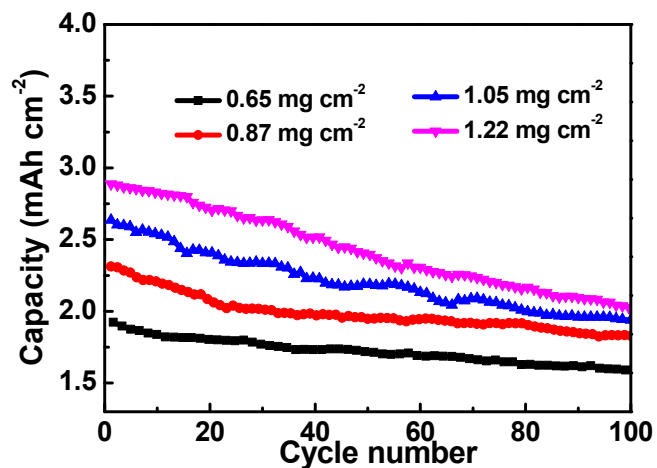


**Figure S7.** The cycle performance of SiNPs electrodes with different mass loading using PAA-FREP binder.

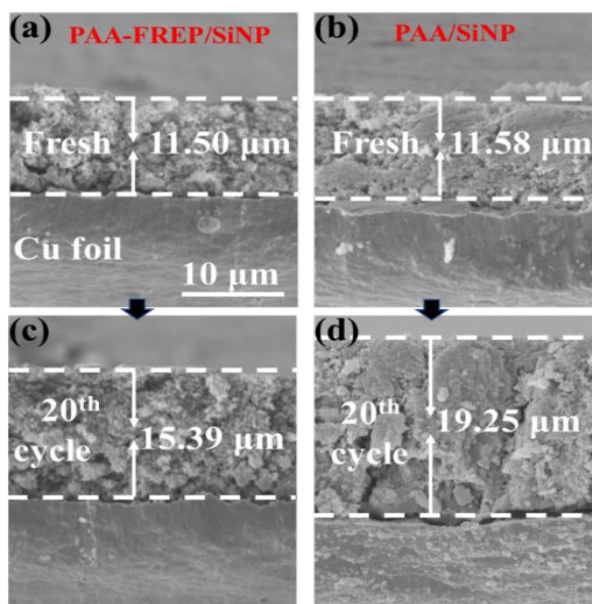


**Figure S8.** Cross-sectional SEM images of SiNPs electrodes before (upper) and after (lower) 20 cycles. Using PAA-FREP (left) and PAA (right) binders.

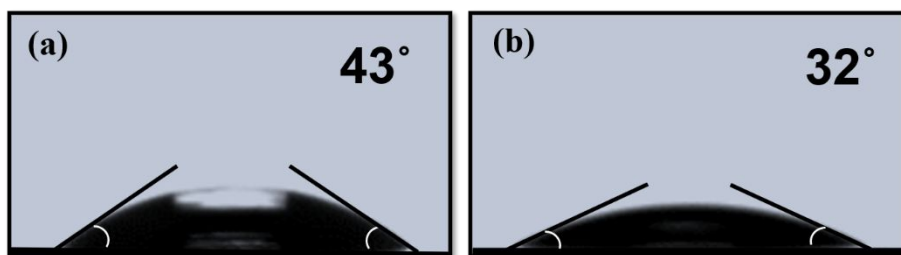


**Figure S9.** Contact angles of  $\text{LiPF}_6/\text{EC-DMC-FEC}$  electrolyte on (a) PAA film and (b) PAA-FREP film.

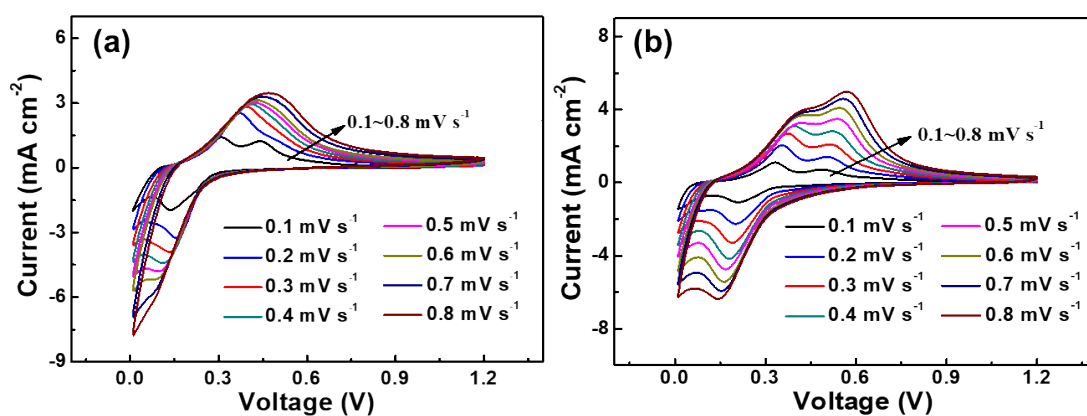


**Figure S10.** CVs of the SiNPs anodes. Using (a) PAA and (b) PAA-FREP binders between 0.01 and 1.2 V at different scan rates.

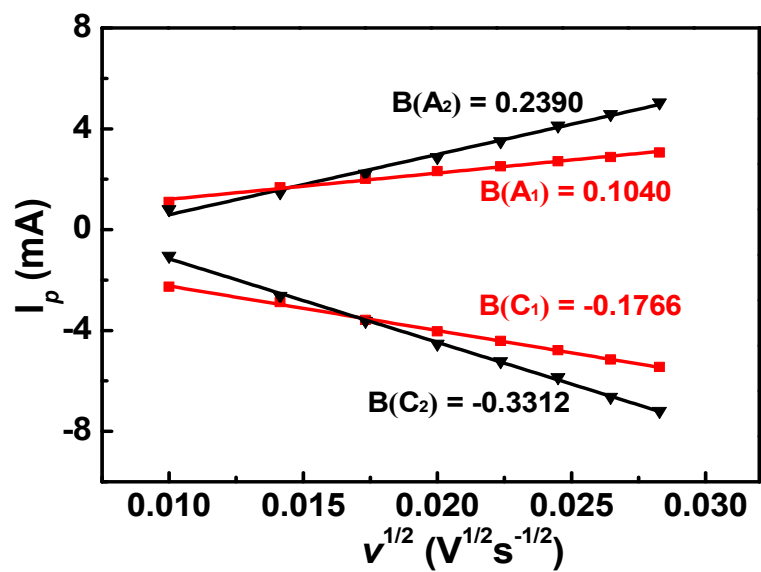


**Figure S11.** Linear fits for the anodic and cathodic peak currents versus scan rates of SiNPs electrodes using PAA-FREP (black) and PAA (red).

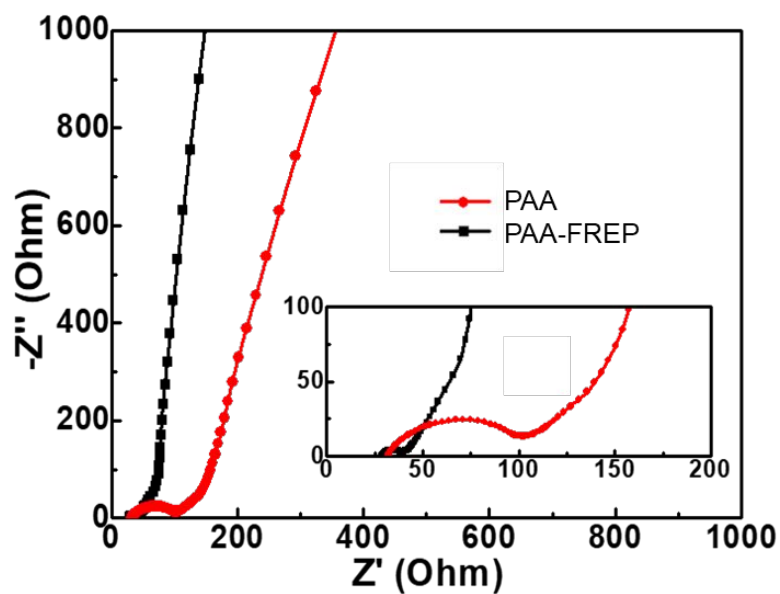


**Figure S12.** EIS of cells with SiNPs electrodes using PAA-FREP and PAA binders after 50 cycles.

---

**Table S1.** Typical data for PAA and PAA-FREP combustion behaviors

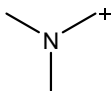
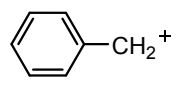
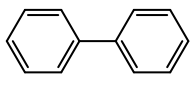
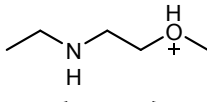
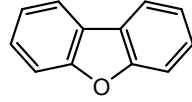
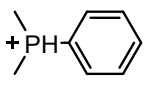
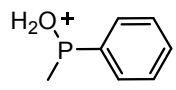
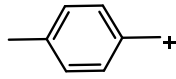
| Binders  | Combustion time (s) | Flame spread | Drip | LOI data(%) |
|----------|---------------------|--------------|------|-------------|
| PAA      | 43.2                | Yes          | Yes  | 18.2        |
| PAA-FREP | 0.2                 | No           | No   | 23.6        |

**Table S2.** TG data of PAA and PAA-FREP in air

| Samples  | T <sub>-5%</sub> (°C) | T <sub>-50%</sub> (°C) | T <sub>max</sub> (°C) | Char residue (%) at 550 °C |
|----------|-----------------------|------------------------|-----------------------|----------------------------|
| PAA      | 192                   | 363                    | 316, 517              | 0                          |
| PAA-FREP | 172                   | 378                    | 251                   | 21.6                       |



**Table S3.** Structural assignments of FREP in the Py-GC-MS.

| m/z | time(min) | structure   |
|-----|-----------|---|
| 58  | 1.697     |    |
| 91  | 6.135     |    |
| 154 | 14.25     |    |
| 154 | 14.362    |     |
| 168 | 16.037    |    |
| 139 | 16.037    |   |
| 141 | 16.037    |  |
| 105 | 18.098    |  |